RESEARCH ARTICLE | FEBRUARY 14 2024

Material gradation effects on twisting statics of bi-directional functionally graded micro-tubes

Reza Aghazadeh ; Mohammad Rafighi ; Raman Kumar ; Mohammed Al Awadh

AIP Advances 14, 025228 (2024)
https://doi.org/10.1063/5.0194270

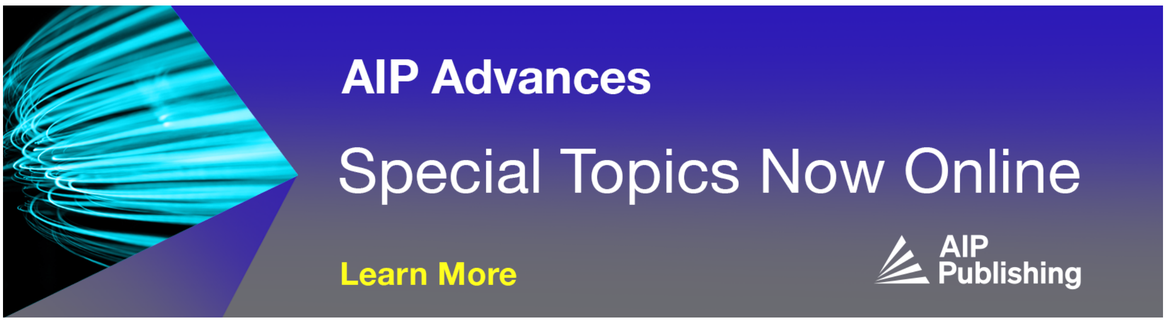

AIP Advances ARTICLE pubs.aip.org/aip/adv

Material gradation effects on twisting statics of bi-directional functionally graded micro-tubes

Cite as: AIP Advances 14, 025228 (2024); doi: 10.1063/5.0194270
Submitted: 26 December 2023 • Accepted: 17 January 2024 •
Published Online: 14 February 2024

Reza Aghazadeh,[1,a)] Mohammad Rafighi,[2,b)] Raman Kumar,[3,c)] and Mohammed Al Awadh[4,d)]

AFFILIATIONS

[1] Department of Aeronautical Engineering, University of Turkish Aeronautical Association, Ankara 06790, Türkiye
[2] Department of Mechanical Engineering, Başkent University, Ankara 06790, Türkiye
[3] Department of Mechanical Engineering, Guru Nanak Dev Engineering College, Ludhiana 141006, India
[4] Department of Industrial Engineering, King Khalid University, Abha 61421, Saudi Arabia

[a)] **Electronic mail:** raghazadeh@thk.edu.tr
[b)] **Author to whom correspondence should be addressed:** mohammad.rafighi@gmail.com
[c)] **Electronic mail:** sehgal91@gndec.ac.in
[d)] **Electronic mail:** mohalawadh@kku.edu.sa

ABSTRACT

This study aims to characterize the twisting behavior of bi-directional functionally graded (FG) micro-tubes under torsional loads within the modified couple stress theory framework. The two material properties involved in the torsional static model of FG small-scale tubes, i.e., shear modulus and material length scale parameter, are assumed to possess smooth spatial variations in both radial and axial directions. Through the utilization of Hamilton's principle, the governing equations and boundary conditions are derived, and then, the system of partial differential equations is numerically solved by using the differential quadrature method. A verification study is conducted by comparing limiting cases with the analytical results available in the literature to check the validity of the developed procedures. A detailed study is carried out on the influences of the phase distribution profile and geometric parameters upon twist angles and shear stresses developed in FG micro-tubes undergoing external distributed torques.

I. INTRODUCTION

In recent years, because of the superior properties of functionally graded materials (FGMs), such as their excellent performance in harsh environments and minimization of stress concentration that rises due to discontinuities in properties of constituent phases, they have become ideal candidates to be used in various technological applications. This new class of inhomogeneous composite materials possesses predetermined smooth spatial variations in volume fractions of components in order to combine the best properties of two distinct constituents, and hence, they can be optimized for a specific purpose. Although FGMs were first used in the aerospace industry as thermal barriers,[1,2] at present, their applications have spread to different industries, such as biomedicine[3,4] and electronics.[5] Recently, along with developments in FGM manufacturing techniques,[6–8] these advanced composites have been widely used in micro- and nano-electromechanical systems (MEMS and NEMS) in the form of small-scale beams, plates, shells, and tubes. Consequently, mechanical analyses of functionally graded (FG) small-scale structures have broadly attracted researchers' attention.

It is experimentally evidenced by several studies[9–12] that classical elasticity approaches are insufficient to capture scaling effects, i.e., when the size gets smaller, conventional continuum theories fail to predict the mechanical behavior correctly; therefore, higher order continuum models have been developed, which utilize length scale parameters to address the side effects.[13–18] One of these nonclassical theories commonly used in mechanical analyses of small-scale structures is the modified couple stress theory (MCST) proposed by Yang *et al.*[18] In this theory, the effects of curvature tensor as a strain gradient measure are also considered in evaluating strain energy besides classical deformation gradient measures. MCST employs a single-length scale parameter to construct the higher-order constitutive relation.

Based on nonclassical theories, numerous studies in the technical literature focus on different small-scale structural problems, such as extensional, flexural, and torsional statics and dynamics of micro- and nano-components. The characterization of the mechanical behavior of FG micro- and nano-tubes/micro- and nano-rods under torsional loading is one of these fundamental problems that, because of their growing applications in MEMS and NEMS, have gained high interest recently.[19–21] Some studies have been devoted to investigating the torsional statics and dynamics of small-scale tubes made of homogeneous materials using strain gradient theory,[22] MCST,[23–25] and nonlocal elasticity theory.[26–28] Fang *et al.*[29] studied the temperature and size effects on the torsional characteristics of a graphene nanoribbon encapsulated in a single-walled carbon nano-tube by performing molecular dynamics simulations.

In most studies on the torsion of FG small-scale tubes, material gradation has been considered to occur only through the radius. Models for predicting twisting and vibrations of radially FG nano-tubes based on nonlocal elasticity are presented by some authors.[30–32] Setoodeh *et al.*[33] utilized MCST to put forward an analytical approach for linear and nonlinear torsional free vibrations of FG micro-/nano-tubes. In another work, MCST is used by Rahaeifard[34] to assess the statics and dynamics of through-radius FG micro-bars.

In recent years, along with advances in FGM processing techniques, the smooth gradation of constitutional phases in two or three dimensions has become feasible, yielding structures with enhanced properties and high applicability. As a result, structural problems involving two- or three-dimensional FG micro-tubes have gained significant interest recently. Various studies exist on the mechanics of two-dimensionally FG large-scale beams, plates, and cylinders based on classical elasticity theory.[35–39] However, a limited number of studies examine the torsional behavior of bi-directional FG micro-tubes. In a study by Barretta *et al.*,[40] based on Eringen's nonlocal elasticity theory, the torsion of viscoelastic circular nano-beams possessing radially quadratic and arbitrary axial distributions of material properties is investigated, and in another study based on a nonlocal elasticity approach, Li and Hu[41] examined the torsional free vibrations of nano-tubes with continuous material gradation in axial and radial directions. In another study by Li and Hu,[42] within the framework of MCST, a procedure to evaluate the angle of rotation and shear stress distribution in bi-directional FG micro-tubes is proposed.

All studies mentioned above disregarded the variation of length scale parameters through the FG medium, which is a simplifying assumption. Experimental studies conducted by some researchers revealed that length scale parameters are material properties.[43–46] A few studies demonstrate the required devices and setups for the experimental determination of length scale parameter values.[47] For instance, the length scale parameter employed in the modified couple stress theory is defined as the square root of the ratio of the modulus of curvature to the shear modulus.[45,46] Both the modulus of curvature and shear modulus are material constants, suggesting that the length scale parameter itself is a material property. Another example is provided by Nikolov *et al.*,[43] who illustrated the dependency of the material length scale parameter in polymers on cross-link density, chain interactions, and chain stiffness, all of which are microstructural properties of the constituent. Consequently, FGM gradation rules must also be applied for these parameters. Although there exist a limited number of studies that treat small-scale parameters as material properties for analyzing beams[48,49] and plates,[50–53] to our best knowledge, no endeavor is reported on torsion of FG micro-tubes with variable length scale parameters in the literature. Accordingly, the current study seems to be the first effort to regard the length scale parameter utilized in MCST as a material constant in modeling torsional statics of FG small-scale tubes.

The current study aims to present an MCST-based model for predicting twisting characteristics of bi-directional micro-tubes under torsional loads. All material properties, including shear modulus and length scale parameters, obey power-law and exponential distribution schemes in radial and longitudinal directions. Hamilton's principle is employed to derive a system of equations governing torsional statics of two-dimensionally FG small-scale tubes. The system is numerically solved using the differential quadrature method (DQM). Parametric studies are carried out to illustrate the influences of different geometric and material features on the angle of rotation and shear stress distribution of FG micro-tubes under externally applied distributed torques.

II. THEORETICAL PRELIMINARIES

According to MCST,[18] the total strain energy U for a linearly elastic, deformable, isotropic material occupying volume Ω is expressed as follows:

$$U = \frac{1}{2}\int_{\Omega} (\sigma_{ij}\varepsilon_{ij} + m_{ij}\chi_{ij})dV, \quad (1)$$

where ε_{ij}, χ_{ij}, σ_{ij}, and m_{ij} represent the components of strain tensor, symmetric curvature tensor, Cauchy stress tensor, and the deviatoric part of couple stress tensor, respectively. ε_{ij} and χ_{ij} are the first- and second-order deformation gradient measures, respectively, which are expressed in terms of displacement field through the following relations:

$$\varepsilon_{ij} = \frac{1}{2}(u_{i,j} + u_{j,i}), \quad (2a)$$

$$\chi_{ij} = \frac{1}{2}(e_{ipq}\varepsilon_{qj,p} + e_{jpq}\varepsilon_{qi,p}). \quad (2b)$$

Here, e_{ijk} represents the components of alternating tensor and the comma stands for differentiation. u_i (i = 1, 2, 3) designate the displacement field of the bi-directional FG micro-tube at time t, and for tubes undergoing torsion, they can be written in the following form:

$$u_1 = 0, \quad (3a)$$

$$u_2(x_1, x_3, t) = -x_3\psi(x_1, t), \quad (3b)$$

$$u_3(x_1, x_2, t) = x_2\psi(x_1, t). \quad (3c)$$

Note that displacements of any point along x_1, x_2, and x_3 directions are, respectively, denoted by u_1, u_2, and u_3. $\psi(x_1,t)$ designates the

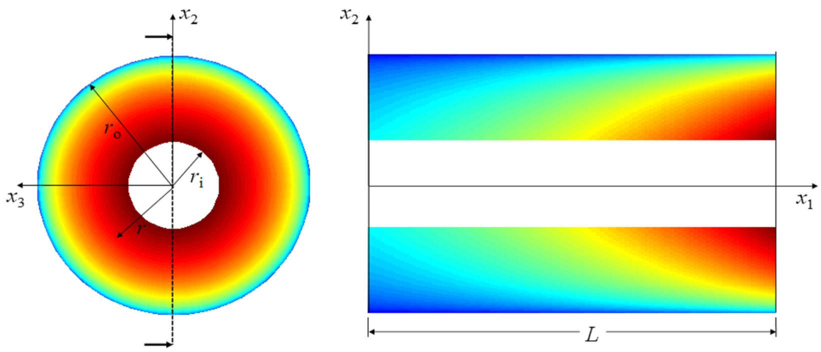

FIG. 1. Configuration of radially and axially FG tubes.

rotation angle about the center of twist, located on the x_1-axis for the axisymmetric configuration considered in the current study. The coordinate system and spatial variations in material properties for a typical two-dimensional FG tube with length L, inner radius r_i, and outer radius r_o are shown in Fig. 1.

Incorporation of Eqs. (3a)–(3c) into Eqs. (2a) and (2b) leads to the following non-zero components of ε_{ij} and χ_{ij}:

$$\varepsilon_{12} = \varepsilon_{21} = -\frac{1}{2}x_3\frac{\partial\psi}{\partial x_1}, \varepsilon_{13} = \varepsilon_{31} = \frac{1}{2}x_2\frac{\partial\psi}{\partial x_1}, \tag{4a}$$

$$\begin{gathered}\chi_{11} = \frac{\partial\psi}{\partial x_1}, \chi_{22} = -\frac{1}{2}\frac{\partial\psi}{\partial x_1}, \chi_{33} = -\frac{1}{2}\frac{\partial\psi}{\partial x_1},\\ \chi_{12} = \chi_{21} = -\frac{1}{4}x_2\frac{\partial^2\psi}{\partial x_1^2}, \chi_{13} = \chi_{31} = -\frac{1}{4}x_3\frac{\partial^2\psi}{\partial x_1^2}.\end{gathered} \tag{4b}$$

Classical and nonclassical stresses are expressed through the use of associated constitutive relations given by

$$\sigma_{12} = \sigma_{21} = -\mu x_3\frac{\partial\psi}{\partial x_1}, \sigma_{13} = \sigma_{31} = \mu x_2\frac{\partial\psi}{\partial x_1}, \tag{5a}$$

$$m_{ij} = 2\mu l^2\chi_{ij}, \tag{5b}$$

where μ is the shear modulus and l is the material length scale parameter.

III. DERIVATION OF THE GOVERNING EQUATIONS

The system of partial differential equations and boundary conditions governing the size-dependent torsional statics of bi-directional FG micro-tubes are derived by employing Hamilton's principle, which postulates that

$$\delta\int_{t_1}^{t_2}(W-U)dt = 0. \tag{6}$$

Here, W denotes the work done by external forces. In the present study, a distributed torque T_e is considered as the external force whose work is given by

$$W = \int_o^L T_e(x_1)\psi dx_1. \tag{7}$$

The continuous variations in constituent phases of the bi-directional FG micro-tube considered in the current study are captured by utilizing two FGM indices, α and β, for axial, x_1, and radial, r, directions, respectively. The material gradation is an exponential function of x_1 and obeys a power-law function along r. Consequently, a typical material property represented by Z, including μ and l, is expressed in the following form:[41]

$$\begin{gathered}Z(r,x_1) = Z_r(r)Z_{x_1}(x_1),\\ Z_{x_1}(x_1) = \exp\left(\frac{\alpha x_1}{L}\right), Z_r(r) = (Z_{li}-Z_{lo})\left(\frac{r_o-r}{r_o-r_i}\right)^\beta + Z_{lo},\\ Z_{ri} = \exp(\alpha)Z_{li}, Z_{ro} = \exp(\alpha)Z_{lo}.\end{gathered} \tag{8}$$

Note that subscripts "*li*," "*lo*," "*ri*," and "*ro*" in Eq. (8) are used to identify left inner ($x_1 = 0, r = r_i$), left outer ($x_1 = 0, r = r_o$), right inner ($x_1 = L, r = r_i$), and right outer ($x_1 = L, r = r_o$) edges, respectively.

Substituting the strain energy U and work W into Eq. (6) yields the following governing equation:

$$\begin{gathered}J_{55}\frac{\partial}{\partial x_1}\left(\mu_{x_1}\frac{\partial\psi}{\partial x_1}\right) + 3A_{552}\frac{\partial}{\partial x_1}\left(\left(\mu l^2\right)_{x_1}\frac{\partial\psi}{\partial x_1}\right)\\ -\frac{1}{4}J_{552}\frac{\partial^2}{\partial x_1^2}\left(\left(\mu l^2\right)_{x_1}\frac{\partial^2\psi}{\partial x_1^2}\right) + T_e = 0.\end{gathered} \tag{9}$$

The boundary conditions are obtained as

$$\begin{gathered}\psi = 0 \text{ or } J_{55}\mu_{x_1}\frac{\partial\psi}{\partial x_1} + 3A_{552}\left(\mu l^2\right)_{x_1}\frac{\partial\psi}{\partial x_1}\\ -\frac{1}{4}J_{552}\frac{\partial}{\partial x_1}\left(\left(\mu l^2\right)_{x_1}\frac{\partial^2\psi}{\partial x_1^2}\right) = 0,\end{gathered} \tag{10a}$$

$$\frac{\partial\psi}{\partial x_1} = 0 \text{ or } \frac{1}{4}J_{552}\left(\mu l^2\right)_{x_1}\frac{\partial^2\psi}{\partial x_1^2} = 0. \tag{10b}$$

Note that in this study, the length scale parameter l is also assumed to be a material property; hence, μl^2 used in the higher order constitutive relation given by Eq. (5b) is considered a distinct material property. As a result, Eq. (8) must also be applied for μl^2, which yields

$$\mu l^2 = \left(\mu_r(r)l_r(r)^2\right)\left(\mu(x_1)l(x_1)^2\right) = \left(\mu l^2\right)_r\left(\mu l^2\right)_{x_1}. \tag{11}$$

TABLE I. Comparison of the maximum angle of rotation $\psi_{\max}$ ($\times 10^{-4}$ rad) and the maximum shear stress $\tau_{\max}$ (MPa) for radially FG micro-tubes, with $l_{lo} = l_{li}$, $\alpha = 0.0$, and $T_0 = 0.5$ N m/m.

	$\psi_{\max}$ ($\times 10^{-4}$ rad)		$\tau_{\max}$ (MPa)	
β	Present	Analytical[42]	Present	Analytical[42]
0.0	7.1574	7.1574	44.9713	44.9713
0.5	4.2003	4.2003	70.9268	70.9268
1.0	3.5491	3.5491	59.9304	59.9304
2.0	3.1221	3.1221	52.7192	52.7192
10.0	2.7481	2.7481	46.4040	46.4040

The stiffness and inertia terms appearing in Eqs. (9) and (10) can be evaluated by

$$J_{55} = \int_A \mu_r \left(x_2^2 + x_3^2\right) dA = \int_A \mu_r r^2 dA = 2\pi \int_{r_i}^{r_o} \mu_r r^3 dr, \tag{12a}$$

$$\{A_{552}, J_{552}\} = \int_A \left(\mu l^2\right)_r \left\{1, \left(x_2^2 + x_3^2\right)\right\} dA = \int_A \left(\mu l^2\right)_r \{1, r^2\} dA = 2\pi \int_{r_i}^{r_o} \left(\mu l^2\right)_r \{r, r^3\} dr, \tag{12b}$$

where A is the cross-sectional area.

IV. METHOD OF SOLUTION

The system of partial differential equations can be solved using the differential quadrature method (DQM). According to DQM, the mth derivative of the angle of rotation ψ at any grid point along the x_1 direction, x_{1i}, can be approximated by a weighted sum of ψ values at all grid points,

$$\frac{\partial^m \psi(x_1)}{\partial x_1^m}\Big|_{x_1 = x_{1i}} = \sum_{j=1}^{N} c_{ij}^{(m)} \psi(x_{1j}) \text{ for } i = 1, 2, \ldots, N, \tag{13}$$

where $c_{ij}^{(m)}$ are the DQM weighting coefficients for the mth derivative and N is the number of grid points. Chebyshev nodes

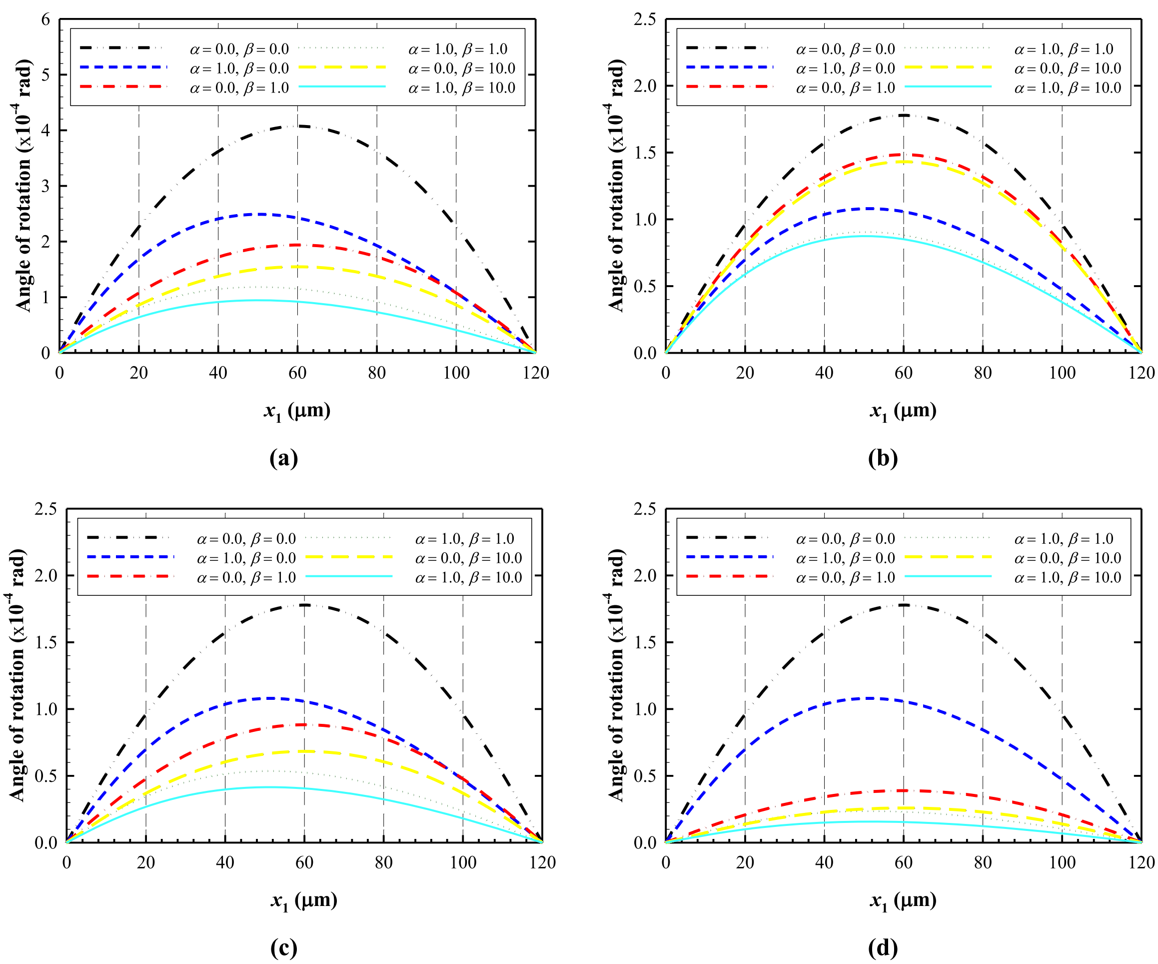

FIG. 2. Angle of rotation of the bi-directional FG micro-tube when (a) $l_{lo} = l_{li} = 0$, (b) $l_{lo}/l_{li} = 0.2$, (c) $l_{lo}/l_{li} = 1.0$, and (d) $l_{lo}/l_{li} = 2.0$.

are used to discretize the tube in a longitudinal direction as follows:

$$x_{1j} = \frac{L}{2}\left\{1 - \cos\left(\frac{\pi(j-1)}{N-1}\right)\right\} \text{ for } j = 1,2,\ldots,N. \tag{14}$$

By utilizing DQM formulated in Eq. (13), the governing equations and boundary conditions are recast into the following system of linear algebraic equations:

$$\mathbf{D}\Psi + \mathbf{Q} = \mathbf{0}, \tag{15}$$

where $\mathbf{D}$ is known as the coefficient matrix, $\mathbf{Q}$ is the forcing vector resulting from the distributed torque, and Ψ is an unknown angular displacement vector containing ψ values at all grid points,

$$\Psi = \{\psi_p\}, \quad p = 1,2,\ldots,N. \tag{16}$$

V. NUMERICAL RESULTS

Here, the numerical results regarding the twisting statics of two-dimensionally FG micro-tubes with both ends fixed are generated and analyzed. The boundary conditions for a fixed-fixed tube can be written as

$$\psi = 0 \text{ at } x_1 = 0, L, \tag{17a}$$

$$\frac{\partial^2\psi}{\partial x_1^2} = 0 \text{ at } x_1 = 0, L. \tag{17b}$$

The bi-directional FG tube, which is considered for parametric investigations in the current study, is made of a metal phase [aluminum (Al) with μ_{li} = 48 GPa] at the left inner edge and a ceramic phase [silicon carbide (SiC) with μ_{lo} = 129 GPa] at the left outer edge. The distribution of length scale parameters is achieved through the ratio l_{lo}/l_{li}. Different distribution patterns for l can be generated by changing this ratio, which can reveal the influence of variable length scale parameters upon numerical results. Using $l_{lo}/l_{li} \neq 1$

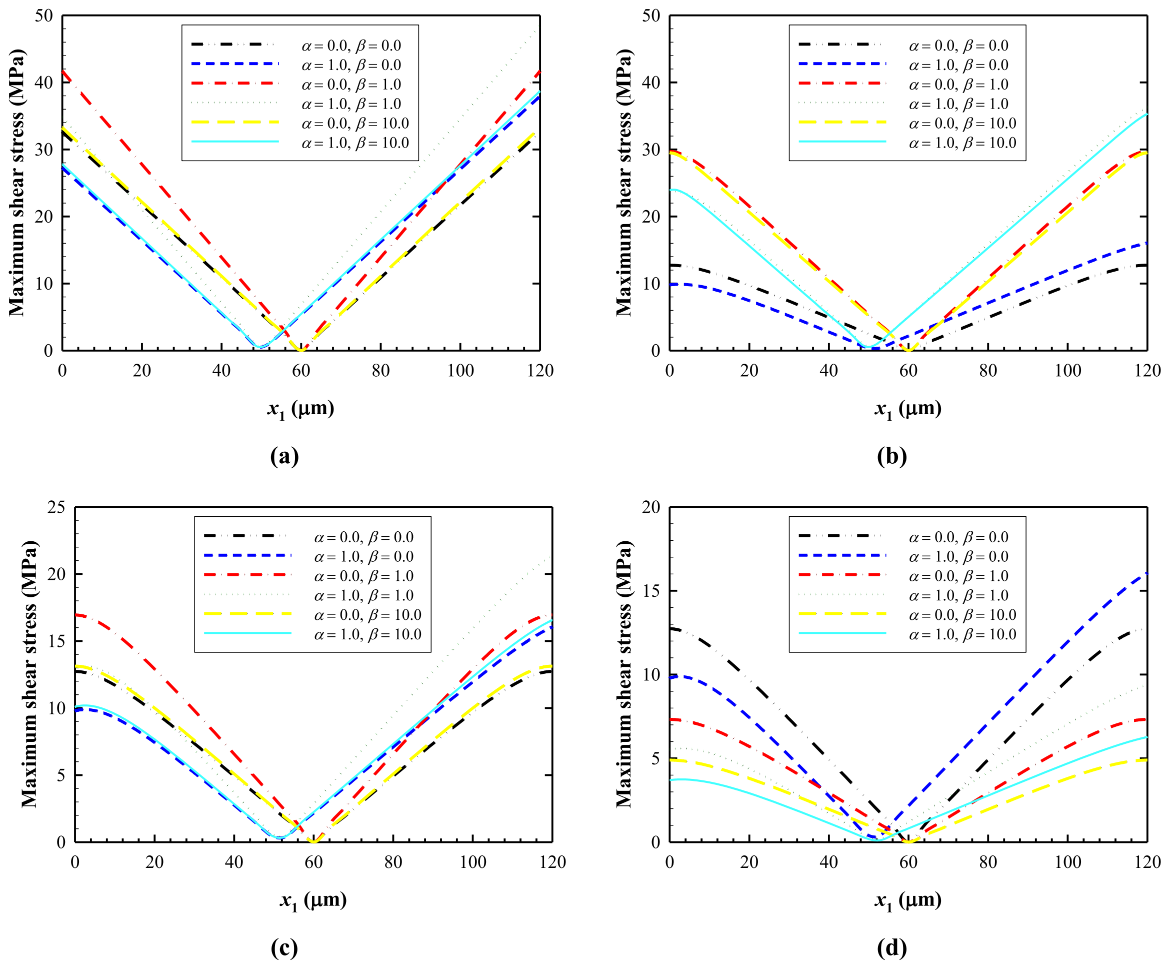

FIG. 3. Maximum shear stress of the bi-directional FG micro-tube when (a) $l_{lo} = l_{li} = 0$, (b) $l_{lo}/l_{li} = 0.2$, (c) $l_{lo}/l_{li} = 1.0$, and (d) $l_{lo}/l_{li} = 2.0$.

along with non-zero values for α and β, the variations of the length scale parameter in radial and axial directions can be captured. $l_{lo}/l_{li} = 1$ and $\alpha = 0$ indicate a constant length scale parameter for the whole bi-directional FG tube.

The geometric dimensions of the micro-tube are illustrated in Fig. 1. Unless otherwise mentioned, the inner and outer radii and the length are taken as $r_o = 50$ μm, $r_i/r_o = 1/2$, and $L = 120$ μm. In order to keep the length scale parameter around geometric dimensions, its value is related to the outer radius as $r_o/l_{li} = 2$. A uniformly distributed torque $T_e = 0.1$ N m/m is used as external loading.

Table I shows the maximum angle of rotation $\psi_{\max}$ and maximum shear stress $\tau_{\max}$ for radially FG micro-tubes compared to the results given by Li and Hu.[42] In their study, Li and Hu[42] provided analytical expressions for the angle of rotation and shear stresses of the radially FG micro-tube ($\alpha = 0$) with constant length scale parameters undergoing a sinusoidally distributed torque $T_e(x_1) = T_0 \sin(\pi x_1/L)$. An excellent correspondence is observed, indicating the accuracy of the procedures developed in the current study. Note that the magnitude of shear stress τ at any point can be evaluated as

$$\tau = \sqrt{\sigma_{12}^2 + \sigma_{13}^2} = \sqrt{\left(-\mu x_3 \frac{\partial \psi}{\partial x_1}\right)^2 + \left(\mu x_2 \frac{\partial \psi}{\partial x_1}\right)^2} = \sqrt{\left(\mu \frac{\partial \psi}{\partial x_1}\right)^2 \left(x_3^2 + x_2^2\right)} = \mu r \frac{\partial \psi}{\partial x_1}. \quad (18)$$

From Eq. (18), it is evident that, at any axial distance, $\tau_{\max}$ occurs on the outer surface, $r = r_o$.

Figure 2 illustrates the through-the-length variation of the rotation angle for different values of FGM indices α and β. Each plot in Fig. 2 is generated using different ceramic-to-metal length scale parameter ratio values l_{lo}/l_{li} while keeping l_{li} constant. The provided results indicate that larger values of l_{lo}/l_{li}, which indicate a larger equivalent length scale parameter, lead to stiffer tubes with small values of twist angle. It can also be observed that an increase in the values of α, or β, or both results in a lower angle of rotation.

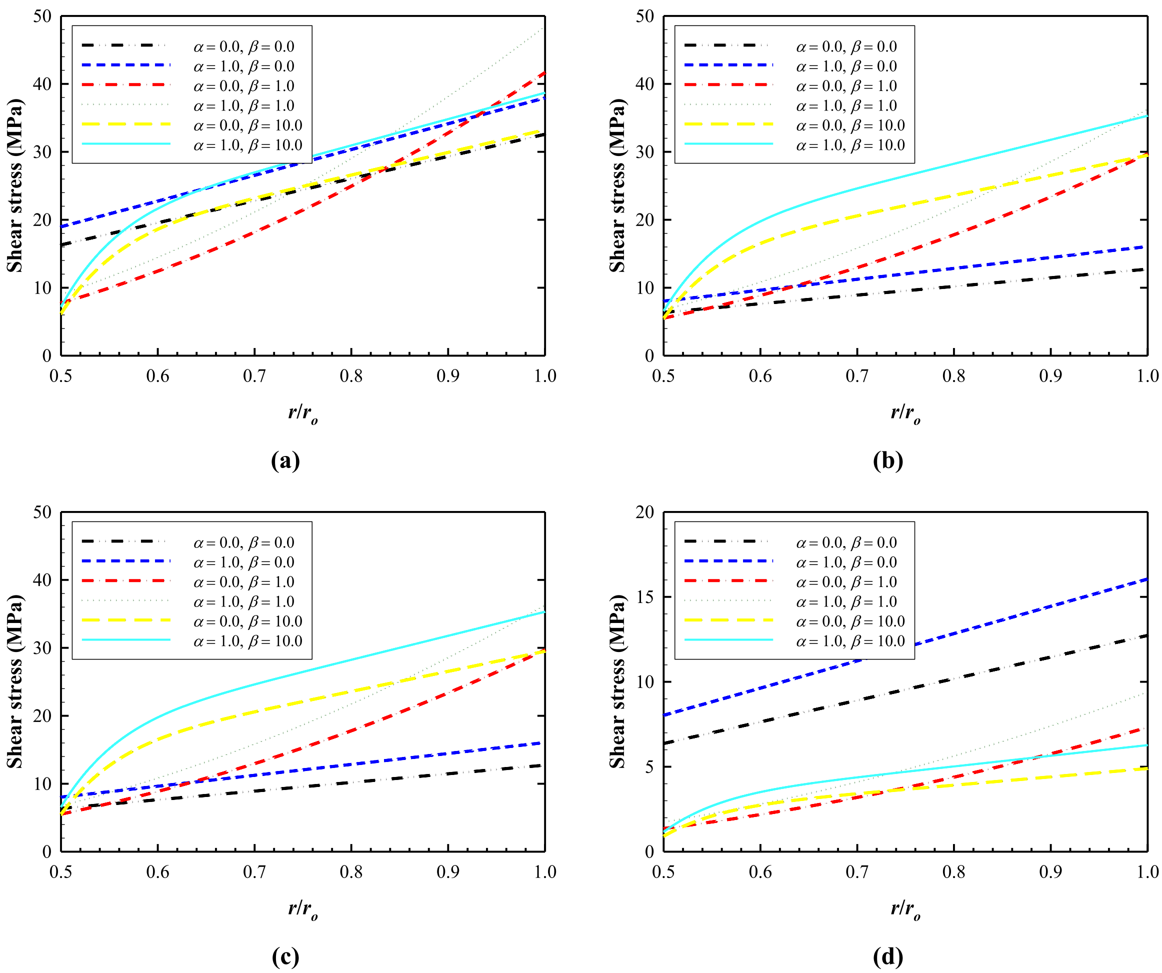

FIG. 4. Shear stress distribution through the radius of the bi-directional FG micro-tube at $x_1 = L$ when (a) $l_{lo} = l_{li} = 0$, (b) $l_{lo}/l_{li} = 0.2$, (c) $l_{lo}/l_{li} = 1.0$, and (d) $l_{lo}/l_{li} = 2.0$.

This fact can be justified by knowing that as α and β get larger, the tube becomes ceramic-rich with a higher equivalent value of shear modulus. For homogeneous or radially FG tubes, due to the length-independent material distribution, the maximum value of ψ is seen to be computed at the midspan, $x_1 = L/2$. However, for axially FG tubes whose α is non-zero, the location of ψ_{max} tends to the left side, which possesses poor material properties with respect to the ones on the right-hand side. By letting $\beta = 0$, through-the-radius variations in volume fractions are neglected, yielding the same distribution profile for l regardless of the l_{lo}/l_{li} value. Thus, the results of zero-β values in Figs. 2(b)–2(d) are equal to each other.

Through-the-length distribution of maximum shear stresses τ_{max}, which occurs at $r = r_o$, is depicted in Fig. 3. Although for $\alpha = 0$, the τ_{max} profile is symmetric about mid-section with a minimum value at $x_1 = L/2$, for non-zero values of α, maximum values of τ_{max} are observed at the right end, and the location of minimum shear stress is shifted to the left. Similar to the conclusion made for Fig. 2, the cases with $\beta = 0$ in Figs. 3(b)–3(d) are unaffected by the change in l_{lo}/l_{li}. Further inspection of Fig. 3 reveals that a rise in β while keeping α as constant results in a drop in the magnitude of τ_{max}. However, by increasing α at a constant β-value, the maximum shear stress on the left- and right-hand sides becomes smaller and larger, respectively.

The radial distribution of shear stress τ at $x_1 = L$, where its maximum value occurs, for different FGM indices α and β is provided in Fig. 4. For only-axially FG micro-tubes, i.e., when $\beta = 0$, the radial distribution is linear, whereas a non-zero β introduces nonlinearity in the distribution profile of shear stress along the radial direction. It can also be seen that, at a constant β-value, higher α-values result in a corresponding increase in τ at the right end.

Figure 5 illustrates the variation of the maximum rotation angle concerning r_o/l_{li} for classical, i.e., $l_{lo} = l_{li} = 0$, and nonclassical, i.e., $l_{lo}/l_{li} = 2$, bi-directional FG tubes. The axial FGM index is kept constant as $\alpha = 0.5$, and three different radial FGM index β values are used to produce the results. Note that, in Fig. 5, to change the value of r_o/l_{li}, the value of l_{li} is altered and r_o is taken as constant. The sensitivity of ψ_{max} to the changes in the values of length scale parameters of phases is observed to be dramatically pronounced as l_{li} gets larger than or close to r_o. However, increasing r_o/l_{li} leads to a corresponding rise in the maximum angle of rotation converging to those predicted by the classical continuum theory.

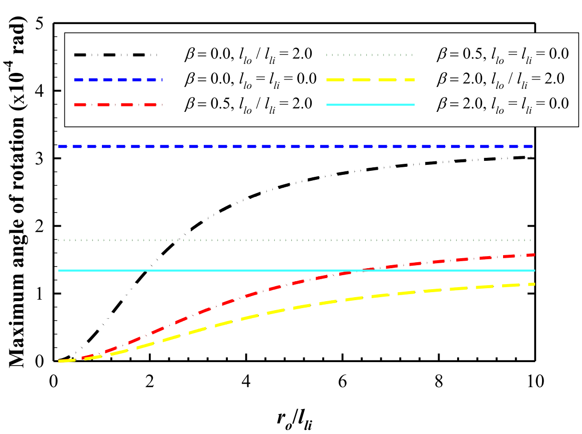

FIG. 5. Maximum angle of rotation of the bi-directional FG micro-tube with $\alpha = 0.5$.

VI. CONCLUDING REMARKS

The current study presents a model and analysis procedures for the torsional statics of bi-directional FG micro-tubes based on the modified couple stress theory. The proposed methods allow consideration of variations of the material properties, including the length scale parameter, through both radial and axial directions. In order to solve a system of governing equations and boundary conditions, a differential quadrature technique is employed. The accuracy of the developed procedures is verified by making comparisons of certain limiting cases to the results available in the literature. The numerical results include through-the-length and through-the-radius distributions of shear stresses and angles of rotation for different values of length scale parameters and FGM indices.

The length scale parameter ratio l_{lo}/l_{li} determines the length scale parameter distribution pattern in a bi-directional FG micro-tube. By observing the sensitivity of the results to this ratio, it can be concluded that considering spatial variations of the length scale parameter in a two-dimensional FG micro-tube is indispensable for the sufficiently accurate prediction of the twisting behavior.

The results also show that FG indices α and β, which characterize the phase distribution profile, significantly influence the torsional statics of the FG tubes. The proposed model and results capture these effects, which can be utilized as a powerful means for design purposes.

The influence of changing the effective value of the length scale parameter to the values with orders close to or beyond the geometrical dimensions of the micro-tube is examined by altering the ratio r_o/l_{li}. From the results provided, it can be found that the larger the effective length scale parameter is, the smaller the rotation angle is. The influence of l on the rotation angle vanishes when it gets sufficiently smaller than geometrical dimensions.

ACKNOWLEDGMENTS

The authors extend their appreciation to the Deanship of Scientific Research at King Khalid University for funding this work through a large group research project under Grant No. RGP2/306/44.

AUTHOR DECLARATIONS

Conflict of Interest

The authors have no conflicts to disclose.

Author Contributions

Reza Aghazadeh: Conceptualization (equal); Investigation (equal); Methodology (equal); Supervision (equal); Validation (equal); Visualization (equal); Writing – review & editing (equal). **Mohammad Rafighi**: Formal analysis (equal); Investigation (equal); Methodology (equal); Validation (equal); Writing – review & editing (equal).

Raman Kumar: Data curation (equal); Project administration (equal); Writing – review & editing (equal). **Mohammed Al Awadh**: Data curation (equal); Resources (equal); Writing – review & editing (equal).

DATA AVAILABILITY

The data that support the findings of this study are available within the article.

REFERENCES

[1] T. Hirai and L. Chen, "Recent and prospective development of functionally graded materials in Japan," Mater. Sci. Forum **308–311**, 509–514 (1999).

[2] S. Uemura, "The activities of FGM on new application," Mater. Sci. Forum **423–425**, 1–10 (2003).

[3] M. Thieme, K.-P. Wieters, F. Bergner, D. Scharnweber, H. Worch, J. Ndop, T. J. Kim, and W. Grill, "Titanium powder sintering for preparation of a porous functionally graded material destined for orthopaedic implants," J. Mater. Sci.: Mater. Med. **12**(3), 225–231 (2001).

[4] A. Tampieri, G. Celotti, S. Sprio, A. Delcogliano, and S. Franzese, "Porosity-graded hydroxyapatite ceramics to replace natural bone," Biomaterials **22**(11), 1365–1370 (2001).

[5] K. Kato, M. Kurimoto, H. Shumiya, H. Adachi, S. Sakuma, and H. Okubo, "Application of functionally graded material for solid insulator in gaseous insulation system," IEEE Trans. Dielectr. Electr. Insul. **13**(2), 362–372 (2006).

[6] A. Witvrouw and A. Mehta, "The use of functionally graded poly-SiGe layers for MEMS applications," Mater. Sci. Forum **492–493**, 255–260 (2005).

[7] Y. Fu, H. Du, and S. Zhang, "Functionally graded TiN/TiNi shape memory alloy films," Mater. Lett. **57**(20), 2995–2999 (2003).

[8] H. Hassanin and K. Jiang, "Net shape manufacturing of ceramic micro parts with tailored graded layers," J. Manuf. Syst. **24**(1), 015018 (2014).

[9] D. C. C. Lam, F. Yang, A. C. M. Chong, J. Wang, and P. Tong, "Experiments and theory in strain gradient elasticity," J. Mech. Phys. Solids **51**(8), 1477–1508 (2003).

[10] J. S. Stölken and A. G. Evans, "A microbend test method for measuring the plasticity length scale," Acta Mater. **46**(14), 5109–5115 (1998).

[11] A. W. McFarland and J. S. Colton, "Role of material microstructure in plate stiffness with relevance to microcantilever sensors," J. Manuf. Syst. **15**(5), 1060 (2005).

[12] N. A. Fleck, G. M. Muller, M. F. Ashby, and J. W. Hutchinson, "Strain gradient plasticity: Theory and experiment," Acta Metall. Mater. **42**(2), 475–487 (1994).

[13] A. C. Eringen, "Nonlocal polar elastic continua," Int. J. Eng. Sci. **10**(1), 1–16 (1972).

[14] M. E. Gurtin, J. Weissmuller, and F. Larche, "The general theory of curved deformable interfaces in solids at equilibrium," Philos. Mag. A **178**, 1093–1109 (1998).

[15] E. C. Aifantis and E. Aifantis, "Strain gradient interpretation of size effects," Int. J. Fract. **95**(1/4), 299–314 (1999).

[16] R. D. Mindlin and H. F. Tiersten, "Effects of couple-stresses in linear elasticity," Arch. Ration. Mech. Anal. **11**(1), 415–448 (1962).

[17] R. A. Toupin, "Elastic materials with couple-stresses," Arch. Ration. Mech. Anal. **11**(1), 385–414 (1962).

[18] F. Yang, A. C. M. Chong, D. C. C. Lam, and P. Tong, "Couple stress based strain gradient theory for elasticity," Int. J. Solids Struct. **39**(10), 2731–2743 (2002).

[19] K. Maenaka, S. Ioku, N. Sawai, T. Fujita, and Y. Takayama, "Design, fabrication and operation of MEMS gimbal gyroscope," Sens. Actuators, A **121**(1), 6–15 (2005).

[20] A. Arslan, D. Brown, W. O. Davis, S. Holmstrom, S. K. Gokce, and H. Urey, "Comb-actuated resonant torsional microscanner with mechanical amplification," J. Microelectromech. Syst. **19**(4), 936–943 (2010).

[21] X. M. Zhang, F. S. Chau, C. Quan, Y. L. Lam, and A. Q. Liu, "A study of the static characteristics of a torsional micromirror," Sens. Actuators, A **90**(1-2), 73–81 (2001).

[22] S. Narendar, S. Ravinder, and S. Gopalakrishnan, "Strain gradient torsional vibration analysis of micro/nano rods," Int. J. Nano Dimens. **3**(1), 1–17 (2012).

[23] B. Gheshlaghi, S. M. Hasheminejad, and S. abbasion, "Size dependent torsional vibration of nanotubes," Physica E **43**(1), 45–48 (2010).

[24] M. Ö. Yayli, "Torsional vibrations of restrained nanotubes using modified couple stress theory," Microsyst. Technol. **24**(8), 3425–3435 (2018).

[25] L. Wang, Y. Y. Xu, and Q. Ni, "Size-dependent vibration analysis of three-dimensional cylindrical microbeams based on modified couple stress theory: A unified treatment," Int. J. Eng. Sci. **68**, 1–10 (2013).

[26] Ç. Demir and Ö. Civalek, "Torsional and longitudinal frequency and wave response of microtubules based on the nonlocal continuum and nonlocal discrete models," Appl. Math. Modell. **37**(22), 9355–9367 (2013).

[27] C. W. Lim, M. Z. Islam, and G. Zhang, "A nonlocal finite element method for torsional statics and dynamics of circular nanostructures," Int. J. Mech. Sci. **94–95**, 232–243 (2015).

[28] M. Arda and M. Aydogdu, "Torsional statics and dynamics of nanotubes embedded in an elastic medium," Compos. Struct. **114**, 80–91 (2014).

[29] T.-H. Fang, W.-J. Chang, Y.-L. Feng, and D.-M. Lu, "Torsional characteristics of graphene nanoribbons encapsulated in single-walled carbon nanotubes," Physica E **83**, 263–267 (2016).

[30] X. Zhu and L. Li, "Twisting statics of functionally graded nanotubes using Eringen's nonlocal integral model," Compos. Struct. **178**, 87–96 (2017).

[31] E. Zarezadeh, V. Hosseini, and A. Hadi, "Torsional vibration of functionally graded nano-rod under magnetic field supported by a generalized torsional foundation based on nonlocal elasticity theory," Mech. Based Des. Struct. Mach. **48**, 480–495 (2019).

[32] Y. Shen, Y. Chen, and L. Li, "Torsion of a functionally graded material," Int. J. Eng. Sci. **109**, 14–28 (2016).

[33] A. R. Setoodeh, M. Rezaei, and M. R. Zendehdel Shahri, "Linear and nonlinear torsional free vibration of functionally graded micro/nano-tubes based on modified couple stress theory," Appl. Math. Mech. **37**(6), 725–740 (2016).

[34] M. Rahaeifard, "Size-dependent torsion of functionally graded bars," Composites, Part B **82**, 205–211 (2015).

[35] D. K. Nguyen, Q. H. Nguyen, T. T. Tran, and V. T. Bui, "Vibration of bi-dimensional functionally graded Timoshenko beams excited by a moving load," Acta Mech. **228**(1), 141–155 (2017).

[36] M. Şimşek, "Bi-directional functionally graded materials (BDFGMs) for free and forced vibration of Timoshenko beams with various boundary conditions," Compos. Struct. **133**, 968–978 (2015).

[37] M. Asgari and M. Akhlaghi, "Natural frequency analysis of 2D-FGM thick hollow cylinder based on three-dimensional elasticity equations," Eur. J. Mech. A **30**(2), 72–81 (2011).

[38] B. Sobhani Aragh and H. Hedayati, "Static response and free vibration of two-dimensional functionally graded metal/ceramic open cylindrical shells under various boundary conditions," Acta Mech. **223**(2), 309–330 (2012).

[39] Q. X. Lieu, D. Lee, J. Kang, and J. Lee, "NURBS-based modeling and analysis for free vibration and buckling problems of in-plane bi-directional functionally graded plates," Mech. Adv. Mater. Struct. **26**(12), 1064–1080 (2019).

[40] R. Barretta, L. Feo, and R. Luciano, "Torsion of functionally graded nonlocal viscoelastic circular nanobeams," Composites, Part B **72**, 217–222 (2015).

[41] L. Li and Y. Hu, "Torsional vibration of bi-directional functionally graded nanotubes based on nonlocal elasticity theory," Compos. Struct. **172**, 242–250 (2017).

[42] L. Li and Y. Hu, "Torsional statics of two-dimensionally functionally graded microtubes," Mech. Adv. Mater. Struct. **26**(5), 430–442 (2019).

[43] S. Nikolov, C. S. Han, and D. Raabe, "On the origin of size effects in small-strain elasticity of solid polymers," Int. J. Solids Struct. **44**(5), 1582–1592 (2007).

[44] R. D. Mindlin, "Second gradient of strain and surface-tension in linear elasticity," Int. J. Solids Struct. **1**(4), 417–438 (1965).

[45] R. D. Mindlin, "Influence of couple-stresses on stress concentrations," Exp. Mech. **3**(1), 1–7 (1963).

[46]S. K. Park and X. L. Gao, "Bernoulli–Euler beam model based on a modified couple stress theory," J. Manuf. Syst. **16**(11), 2355 (2006).
[47]A. Farajpour, H. Farokhi, and M. H. Ghayesh, "Mechanics of fluid-conveying microtubes: Coupled buckling and post-buckling," Vibration **2**(1), 102–115 (2019).
[48]M. H. Kahrobaiyan, M. Rahaeifard, S. A. Tajalli, and M. T. Ahmadian, "A strain gradient functionally graded Euler–Bernoulli beam formulation," Int. J. Eng. Sci. **52**, 65–76 (2012).
[49]R. Aghazadeh, E. Cigeroglu, and S. Dag, "Static and free vibration analyses of small-scale functionally graded beams possessing a variable length scale parameter using different beam theories," Eur. J. Mech. A **46**, 1–11 (2014).
[50]I. Eshraghi, S. Dag, and N. Soltani, "Bending and free vibrations of functionally graded annular and circular micro-plates under thermal loading," Compos. Struct. **137**, 196–207 (2016).
[51]A. Alipour Ghassabi, S. Dag, and E. Cigeroglu, "Free vibration analysis of functionally graded rectangular nano-plates considering spatial variation of the nonlocal parameter," Arch. Mech. **69**(2), 105 (2017).
[52]R. Aghazadeh, S. Dag, and E. Cigeroglu, "Modelling of graded rectangular micro-plates with variable length scale parameters," Struct. Eng. Mech. **65**(5), 573–585 (2018).
[53]R. Aghazadeh, S. Dag, and E. Cigeroglu, "Thermal effect on bending, buckling and free vibration of functionally graded rectangular micro-plates possessing a variable length scale parameter," Microsyst. Technol. **24**(8), 3549–3572 (2018).